Mechanisms of the ultrafast production and recombination of solvated electrons in weakly polar fluids: Comparison of multiphoton ionization and detachment via the charge-transfer-to-solvent transition of Na^- in THF

Ignacio B. Martini, Erik R. Barthel, and Benjamin J. Schwartz[a)]
Department of Chemistry and Biochemistry, University of California, Los Angeles, Los Angeles, California 90095-1569

(Received 24 July 2000; accepted 2 October 2000)

The processes by which solvated electrons are generated and undergo recombination are of great interest in condensed phase physical chemistry because of their relevance to both electron transfer reactions and radiation chemistry. Although most of the work in this area has focused on aqueous systems, many outstanding questions remain, especially concerning the nature of these processes in low polarity solvents where the solvated electron has a fundamentally different structure. In this paper, we use femtosecond spectroscopic techniques to explore the dynamics of solvated electrons in tetrahydrofuran (THF) that are produced in two different ways: ejection by multiphoton ionization of the neat solvent, and detachment via the charge-transfer-to-solvent (CTTS) transition of sodide (Na^-). Following multiphoton ionization of the solvent, the recombination of solvated electrons can be well described by a simple model that assumes electrons are first ejected to a given thermalization distance and then move diffusively in the presence of the Coulombic attraction with their geminate cation. The short-time transient absorption dynamics of the THF radical cation in the visible region of the spectrum do not match the kinetics of the solvated electron probed at $\sim 2\ \mu$m, indicating that caution is warranted when drawing conclusions about recombination based only on the dynamics of the solvent cation absorption. With ~ 4 eV of excess energy, geminate recombination takes place on the hundreds of picoseconds time scale, corresponding to thermalization distances $\geqslant 40$ Å. The recombination of solvated electrons ejected via CTTS detachment of Na^-, on the other hand, takes place on two distinct time scales of $\leqslant 2$ and ~ 200 ps with kinetics that cannot be adequately fit by simple diffusive models. The fraction of electrons that undergo the fast recombination process decreases with increasing excitation energy or intensity. These facts lead us to conclude that electrons localize in the vicinity of their geminate Na atom partners, producing either directly overlapping or solvent-separated contact pairs. The distinct recombination kinetics for the two separate electron generation processes serve to emphasize the differences between them: multiphoton ionization produces a delocalized electron whose wave function samples the structure of the equilibrium fluid before undergoing localization, while CTTS is an electron transfer reaction with dynamics controlled by the motions of solvent molecules adjacent to the parent ion. All the results are compared to recent experiments on the photodetachment of electrons in aqueous systems where contact pairs are also thought to be important, allowing us to develop a qualitative picture for the mechanisms of electron generation and recombination in different solvent environments. © *2000 American Institute of Physics.* [S0021-9606(00)52048-0]

I. INTRODUCTION

Solvated electrons are excess charges in a liquid that are not associated with a single solvent molecule. Instead, these electrons are physically confined in a cavity between solvent molecules and have an electronic structure determined by the cavity's fluctuating size and shape. Because solvated electrons are important in radiation chemistry,[1] serve as intermediates in charge transfer reactions,[2] and provide model systems for understanding the role of quantum dynamics in the condensed phase,[3] they have been the subject of intense study over the past few decades. The outstanding questions to be addressed include the mechanism by which the excess electrons are generated and the manner by which they become localized in the solvent cavity. The initial work in this field addressed these questions by studying the free ion yield of solvated electrons produced using pulse radiolysis.[1] More recently, the advent of tunable ultrafast laser sources has offered the opportunity to observe directly the electron generation and localization processes following multiphoton ionization of the neat liquid.[4–11] Accompanied by quantum simulations,[12] the general picture that has emerged is that the initial step in the photoionization process consists of vertically exciting electrons into the conduction band of the liquid. These initially prepared electrons (which likely correspond to ''dry electrons'' in the literature) resemble plane

a)Author to whom correspondence should be addressed; electronic mail: schwartz@chem.ucla.edu

waves in the conduction band of a solid, but are distorted and localized by the disorder of the fluid. The liquid responds to the presence of the electron by expanding a small cavity where part of the electronic wave function resides; this further localizes the spatial extent of the wave function, leading to formation of a solvated electron. It is also possible that the electron can be trapped in an electronically excited state during the localization process (likely corresponding to the ''wet'' or ''pre-solvated'' electron in the literature); this excited state then relaxes nonradiatively to the ground state, leading to the equilibrium solvated electron.

Following ejection and localization, solvated electrons can undergo diffusive motion, leading to the possibility of recombination with the product species from which the electron was generated (geminate recombination).[13] The average distance at which a photoejected electron localizes from its parent is known as the thermalization length; the more excess energy provided by the photons, the greater the thermalization length. Once ejected and thermalized, the electron and its geminate partner move diffusively (and possibly under the influence of their mutual Coulomb attraction if the partner is charged), so that there is some probability that they recombine.[14] Solvated electrons produced with a greater thermalization length take longer to recombine and have a higher probability for escaping recombination than electrons produced with smaller thermalization lengths. Thus, the kinetics of recombination can be used to learn about the electron ejection process: by using transient absorption spectroscopy to monitor the number of electrons that survive as a function of time, the thermalization length can be inferred.

While the thermalization and recombination kinetics of solvated electrons have been studied in a variety of solvents, by far the most attention has been lavished on aqueous systems.[4–8] For water, once the changing order of multiphoton processes with excitation wavelength is accounted for, it is clear that increasing excitation energy above the ionization threshold leads to an increased thermalization length for the ejected electron.[15] Depending on the excitation energy, recombination typically occurs on a time scale of tens to hundreds of picoseconds. It is also worth noting that the recombination kinetics in aqueous systems is somewhat complicated by the fact that the water cation produced upon photoionization reacts essentially instantaneously with a nearby water molecule to produce H_3O^+ and OH•. The hydrated electron recombines preferentially with the hydroxyl radical; reaction with the hydronium ion serves only as a minor recombination channel.[7,16]

In contrast, quite a bit less is known about electron generation and recombination in nonpolar liquids.[9–11] Without the strong dipolar forces present in polar liquids, solvated electrons in nonpolar fluids tend to occupy much larger volumes than their polar counterparts.[17,18] As a result, the absorption spectrum of solvated electrons in nonpolar and weakly polar solvents tends to peak in the mid-infrared, typically near 2 μm[19] (the absorption maximum of the hydrated electron, for comparison, is 720 nm[20]). The mid-infrared is a wavelength range that was inaccessible to ultrafast lasers until recently; as a result, essentially all of the work in nonpolar fluids has examined recombination dynamics by monitoring the visible-wavelength absorption of the solvent radical cation. For example, Long, Eisenthal and co-workers studied multiphoton ionization in alkanes and, based on the decay of transient absorptions at several visible wavelengths, claimed that geminate recombination in *iso*-octane can take place on a sub-picosecond time scale.[9] This fast geminate recombination can be explained by the higher electron mobility and the lower dielectric constant (which leads to a larger Coulomb force between the electron and cation) of *iso*-octane relative to polar fluids like water. The absorption of solvent radical cations, however, might also change as a result of processes other than changes in cation population: vibrational energy relaxation, solvation dynamics, or free radical chemistry can alter the absorption spectrum on the same time scale(s) as geminate recombination. Thus, for experiments in nonpolar solvents in which the electron is not being probed directly, these other processes that might affect the cation absorption could possibly masquerade as geminate recombination.[10]

In addition to producing solvated electrons by photoionization of the neat solvent, it is also possible to generate solvated electrons by photodetachment of a solute.[21] For example, molecules such as tetramethylphenylene diamine[22] undergo spontaneous ionization following excitation to the first singlet excited state, generating solvated electrons. Recent experiments have found the surprising result that following the photoionization of indole in water, essentially no geminate recombination occurs.[23] Given that the excitation wavelength is usually well below the vertical ionization threshold, so that the thermalization length is expected to be relatively low, this result suggests that there is a large free energy barrier to recombination. A large barrier could be the outcome of having the electron and cation become bound in a solvent-separated contact pair: if the energetic price to disrupt the local solvent structure around the pair is large relative to kT, recombination could be effectively prevented.[23]

The presence of solvated electron:geminate partner contact pairs has also been invoked in yet another example of electrons generated via photodetachment from a solute: that of charge-transfer-to-solvent (CTTS).[24–28] In contrast to the photoejection process described above, simulations have predicted that electron production via CTTS proceeds via a much different mechanism.[29,30] In a CTTS reaction, a photon promotes the electron on an anion in solution to a *localized* excited state (the CTTS state) which is bound not only by the Coulomb attraction between the electron and the anion nucleus but also by the polarization of the solvent around the anion. Following excitation, the local solvent structure around the anion changes, causing the electron to detach and become solvated in a cavity nearby the parent. Thus, the acronym CTTS is somewhat of a misnomer: the Franck–Condon CTTS excitation does not directly produce solvated electrons. For the CTTS process in aqueous halides, simulations suggest that after detachment, the hydrated electron and neutral halogen atom are bound by several kT in a contact pair, separated by only a few angstroms.[30] Once formed, there are two ways for the contact pair to undergo recombi-

nation. If the solvated electron's wave function overlaps that of the nearby partner atom, recombination can occur directly via a nonadiabatic transition; the rate for this type of process can be estimated by the Golden Rule.[30,31] If the solvated electron is held at some distance from its geminate partner, on the other hand, recombination cannot take place until the local solvent structure is disrupted, a situation akin to that of the indole photoionization described above.

Recently, we presented a detailed exploration of the dynamics of electron production following the CTTS excitation of sodide (Na^-) in tetrahydrofuran (THF).[32] Our choice of Na^- was based on the spectroscopic convenience afforded by this system: the spectra of both the CTTS ground and excited states, as well as the absorptions of both the solvated electron and neutral sodium atom products, are easily accessible in the visible or near-infrared. Following excitation, we observed the decay of the CTTS excited state and the corresponding appearance of the solvated electron in $\sim$700 fs. When exciting at 800 nm near the CTTS band maximum, a majority of the electrons produced undergo geminate recombination in less than 2 ps. In order to fit the observed spectral transients, we had to invoke the presence of a contact pair that undergoes a pseudo-first-order recombination process. Bradforth and co-workers recently have carried out a similar set of experiments for the CTTS transition of aqueous iodide.[28] Like we determined for the Na^-/THF system, Bradforth and co-workers also found that the electron dynamics following CTTS detachment from iodide is best described in terms of recombination of a contact pair. In contrast to the rapid, $\leqslant$2-ps recombination observed following CTTS excitation of sodide in THF,[32] recombination in the aqueous iodide system was observed to take place on a time scale of tens of picoseconds.[28]

All of these observations lead to some fundamental questions: Why do the time scales for electron recombination appear to be so much faster in weakly polar fluids like THF than in polar liquids like water? Why is formation of a contact pair important for electrons produced via CTTS but not for electrons generated via multiphoton ionization? Why do contact pairs in water live for so much longer than in low polarity solvents like THF? How does increasing the excitation energy affect contact pair formation following CTTS? How do the observed differences in behavior depend on the interplay between the solute's electronic structure and the solvent dynamics?

The purpose of this paper is to address these and related questions by comparing the production and recombination dynamics of solvated electrons generated by multiphoton ionization to those of solvated electrons produced via CTTS in weakly polar fluids. For solvated electrons produced by multiphoton ionization of THF, we find that recombination occurs on a hundreds of picoseconds time scale with kinetics that are well described by a model assuming ejection at a thermalization length followed by diffusive motion in a Coulomb field. We also find that the absorption dynamics of the solvent cation do not match with those of the solvated electron at early times, showing that at least for the THF system, experiments which probe the cation absorption could erroneously conclude that there are fast recombination kinetics. For electrons produced via CTTS excitation of sodide (Na^-) in THF, we see two time scales for recombination: a fast recombination on $\leqslant$2-ps-time scale, and a slower recombination on a hundreds of picoseconds time scale. Neither of the recombination decays can be adequately described by a diffusive kinetic scheme, pointing to the importance of both directly overlapping and solvent-separated geminate atom: solvated electron contact pairs following CTTS detachment. All of the results emphasize that direct photoejection is a fundamentally different electron production mechanism than CTTS.

II. EXPERIMENT

The solvent we have chosen for this study is THF. Alkali metal anion solutions can be prepared readily in this solvent, and unlike metal/amine solutions, there are no solvated electrons present at equilibrium, allowing us to cleanly monitor the appearance of solvated electrons produced by detachment following CTTS excitation of sodide.[33] Our choice of Na^- as the CTTS anion of interest is based not only on its spectroscopic convenience[32,34] but also on the fact that sodium leached out of the walls of the sample cell can act as a contaminant in solutions of the other alkali metal anions.[35] Our procedure for preparing sodium anions is an adaptation of the method of Dye;[36] the details have been reported in our previous paper.[32] For both the neat solvent and sodide CTTS studies, the THF employed was freshly dried over potassium metal before use. All of the experiments performed on samples with different concentrations of Na^- produced identical results, indicating that interactions between neighboring Na anions are not important in any of the dynamics reported here. It is also well known from conductance measurements that there is essentially no ion pairing between the cations and alkali metal anions in these solutions,[37] so the experiments reported below can be regarded as spectroscopic studies of isolated, uncomplexed Na anions.

The laser system used for the femtosecond pump-probe experiments is a regeneratively amplified Ti:sapphire laser (Spectra Physics) that produces 1 mJ, $\sim$120-fs pulses at 790 nm at a 1-kHz repetition rate. The amplified pulses pump a dual-pass optical parametric amplifier (OPA) that generates tunable signal and idler beams in the infrared. In particular, the idler beam can be tuned through the region near 2 μm, allowing easy spectroscopic access to the absorption of the solvated electron in THF, which has its absorption maximum near 2.1 μm.[19] In addition to using the OPA outputs directly, both the signal and idler beams may pass through additional nonlinear crystals to produce tunable visible pulses via harmonic generation or by sum frequency mixing with the residual 790-nm fundamental light. The probe light in the experiment is split into signal and reference beams, which are detected on a shot-by-shot basis with matched InGaAs or Si photodiodes as appropriate for the wavelength. The system is sensitive enough to measure absorption changes of $\sim$1 mOD averaging as few as 600 laser shots per point; the full details of our pump-probe spectrometer have been described elsewhere.[32,38] The pump beam intensity was controlled

using calibrated neutral density filters. Control experiments on the empty sample container assured that the silica cell walls did not contribute to any of the measured pump-probe signals.

As discussed further below, it is not obvious in the experiments on neat THF how many photons are involved in the multiphoton ionization of the solvent at a given pump wavelength. Thus, to determine the number of photons used to ionize THF, we also measured the intensity dependence of the nonlinear absorbance of neat THF at different pump wavelengths. The setup for this nonlinear absorbance experiment is similar to that recently reported by Crowell and Qian for liquid water.[39] In brief, the energy of a portion of the pump pulse was measured on photodiodes both before and after the THF sample as a function of pump pulse intensity. Calibrated neutral density filters were used to prevent saturation of the diodes at high intensities. Absolute fluences were determined by calibrating the number of counts recorded from the integrated and digitized photodiode signals against a pyroelectric power meter at the highest intensities. The number of photons absorbed in the multiphoton process is then determined by the slope of a log-log plot of absorbance against input intensity.[40]

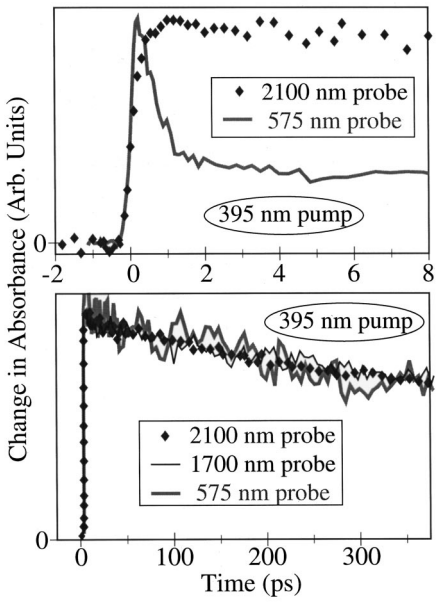

FIG. 1. Femtosecond pump-probe transients exciting neat THF with 395-nm light. Upper panel: The solid diamonds show the appearance of the solvated electron monitored near its absorbance maximum at 2100 nm, the solid curve shows the dynamics of the THF radical cation probed at 575 nm. The two transients have been normalized to have the same maximum change in absorbance. Lower panel: Same data as in the upper panel on a longer time scale, with the transients normalized to have the same change in absorbance at a time delay of 8 ps. The thin solid curve shows the dynamics of the solvated electron detected at 1700 nm.

III. RESULTS

One of the key aspects of this work is that the solvated electron in THF is a fundamentally different object than the solvated electron in water. Many studies have shown that solvated electrons in nonpolar and weakly polar liquids have a much greater spatial extent than electrons in polar fluids like water.[17,18,41,42] In 2-methyltetrahydrofuran glass, electron paramagnetic resonance experiments indicate that the radius of the solvated electron's cavity is $\sim$3.4 Å, and moreover, that only a small fraction of the electron's density is found on the nearest proton sites, implying that the electronic wave function extends out to distances much farther than the first solvent shell.[42] Our picture of the solvated electron in THF is of a quantum mechanical object with the majority of the probability density inside a 3.4 Å diameter cavity, but with tendrils of probability density extending out past the closest solvent molecules. In contrast, the hydrated electron is essentially completely confined within its $\sim$2.0 Å radius cavity.[43] As we will see below, the larger size of solvated electrons in THF has important implications for the recombination behavior, especially for those electrons produced by CTTS excitation that are bound in contact pairs. Thus, in the remainder of this section, we present our results on the recombination dynamics of solvated electrons in THF, first for electrons produced by multiphoton ionization of the neat solvent, and second for electrons produced via detachment following CTTS excitation of Na^-.

A. Electron production by multiphoton ionization of neat THF

In this section, we use femtosecond pump-probe spectroscopy to monitor the survival probability of solvated electrons produced by multiphoton ionization of neat THF. We then fit the observed kinetics to a standard model involving diffusion under the influence of the Coulomb potential. This allows us to extract the thermalization length, which can be correlated with the excess energy if the ionization potential and the number of photons absorbed are known. Unfortunately, the ionization potential of liquid THF is not known: The liquid ionization potential will be lower than the gas phase ionization potential of 9.38 eV[44] because the electronic polarizability of the liquid lowers the energy of the free electron and cation relative to vacuum. Following the recent work of Rozenshtein *et al.* who have studied the photoionization of Rb^- in THF,[45] we can estimate the ionization potential of liquid THF by making use of the Born formula to calculate the polarization energy provided by the solvent. We find that weakly polar fluids such as THF provide $\sim$1.8 eV of polarization energy to lower the liquid ionization potential relative to the gas phase value. It is reasonable to use this $\sim$1.8 eV polarization energy, along with the $\sim$9.4 eV gas phase ionization potential, to estimate that the ionization energy of liquid THF is $\sim$7.6 eV. This means that the multiphoton ionization of neat THF requires at least three 395-nm (3.1 eV) photons, at least four 500-nm (2.5 eV) photons, and at least four or possibly five 575-nm (2.1 eV) photons.

Figure 1 shows the results of femtosecond pump-probe experiments in which neat THF was ionized with 395-nm photons. The upper panel shows the early dynamics in the first few ps, while the lower panel shows the same transients on the hundreds of ps time scale. The dynamics of the solvated electron were probed at both 1700 (thin solid curve) and 2100 nm (solid diamonds); the two transients are indistinguishable within the signal-to-noise. The fact that the dynamics are wavelength-independent indicates that processes

such as solvation dynamics that could shift the solvated electron's absorption spectrum are not important on the time scales considered here.[46] Thus, the amplitude of the absorption near 2 μm provides a direct measure of the population of solvated electrons, and hence the electron's survival probability. Figure 1 makes it clear that following multiphoton ionization at 395 nm, solvated electrons in THF live for hundreds of picoseconds and undergo no appreciable recombination on the few-ps time scale.

Most previous studies of solvated electron recombination dynamics in nonpolar and weakly polar liquids have relied on probing the visible absorption of the solvent radical cation rather than the infrared absorption of the electron because of the limitations of the ultrafast laser sources available at the time.[9–11,47] The heavy solid curves in Fig. 1 show the results of this type of experiment for the 395-nm multiphoton ionization of THF, where the solvent radical cation is probed in the visible at 575 nm. To the best of our knowledge, Fig. 1 represents the first direct comparison of the absorption dynamics of both the cation and electron following multiphoton ionization. The lower panel shows the data normalized to have the same change in absorbance at 8 ps delay; it is clear that the long time decay of the solvent cation absorption matches perfectly with that of the solvated electron,[48] supporting the assignment of this decay to geminate recombination. The upper panel of Fig. 1 shows the same data on shorter time scales, normalized to the maximum change in absorbance. The rapid dynamics of the 575-nm cation transient have no counterpart in the $\sim$2-μm electron signals; thus, the fast decay at 575 nm cannot correspond to geminate recombination. Instead, the fast dynamics probed at 575 nm likely result from vibrational energy relaxation, solvation dynamics, or another process such as an H atom abstraction reaction that alters the cation's absorption spectrum. If the trend we see for the cation dynamics in THF holds true for other liquids, the conclusions of many of the previous studies that investigated only the solvent cation absorption may need to be reassessed.

Figure 2 compares the recombination dynamics of solvated electrons in THF following multiphoton ionization at three different excitation wavelengths: 395 (circles—same as the solid diamonds in Fig. 1), 500 (crosses) and 575 nm (open diamonds). Consistent with the short-time data in Fig. 1, none of the transients shows any evidence for geminate recombination on early time scales. Perhaps more surprising, the longer-time recombination dynamics for the different excitation wavelengths are remarkably similar: The dynamics following 500- and 575-nm excitation are the same within the signal-to-noise, and recombination is only marginally slower for ionization with 395-nm photons (Fig. 2 inset). This leads to some obvious questions, such as: Given that the different excitation wavelengths should provide different amounts of excess energy, why are the recombination dynamics (and hence, the thermalization lengths) so similar for the three cases? And, why are the recombination decays so slow compared to those seen in other fluids like water? The answer to both of these questions lies in determining precisely how many photons are being used in the ionization process at each excitation wavelength.

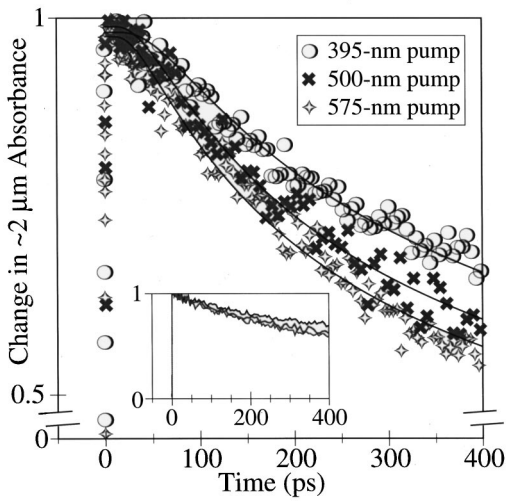

FIG. 2. Dynamics of the solvated electron's absorption at $\sim$2 μm following femtosecond excitation of neat THF at a variety of pump wavelengths: 395 (open circles, same as solid diamonds in Fig. 1), 500 (crosses), and 575 nm (open diamonds). The data are normalized to have the same maximum change in absorbance. The thin solid curves are fits to Eqs. (1) and (2); see text for details. Note that the main figure has a highly expanded vertical scale (there is a scale break at the bottom of the *y* axis). The inset shows the same data as the main figure on an absolute scale.

Unfortunately, we were unable to determine the order of the multiphoton ionization process simply by measuring the change in the size of the electron absorption signal with excitation intensity: For all three excitation wavelengths, the electron signal scaled linearly with pump power. Since the neat THF sample clearly does not absorb only one photon, this linear power dependence must be indicative of a multiphoton process driven into saturation. In addition to the linear power dependence, all of the dynamics presented in Fig. 2 were independent of excitation intensity for the range accessible in this study.[49] In previous work on the multiphoton ionization of water, the recombination dynamics were found to be strongly intensity-dependent at some excitation wavelengths, showing that the order of the multiphoton excitation process can change with pump power.[4,15] The intensity-independence of the results presented in Fig. 2 is again consistent with the idea of a saturated multiphoton process: The intensity would likely have to be lowered below our detection threshold to avoid absorption of the last photon, and the lack of intensity dependence suggests there is little probability to absorb additional photons at the higher excitation intensities within reach.

Thus, instead of trying to determine the number of pump photons absorbed by measuring the electrons that are produced, it makes more sense to measure the number of photons absorbed directly. Figure 3 shows the results of a direct, nonlinear absorbance experiment on neat THF;[39] the inset includes a simplified schematic of the experimental setup, and the main figure shows a typical nonlinear absorbance data set for 575-nm excitation. The data are presented as a log-log plot of the absorbance of the THF sample versus the intensity incident on the sample. The results show at least two different intensity regimes of interest. At the lowest pump intensities, the data on the log-log plot have a slope of

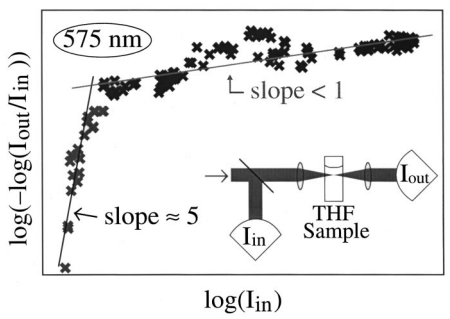

FIG. 3. Nonlinear absorbance of neat THF as a function of intensity for 575-nm excitation. The inset at lower right shows a schematic of the experiment, taken after Ref. 39. The data (crosses) are plotted on a log-log scale; the solid lines are linear least-squares fits to the data with the indicated slopes.

$\sim$5, indicative of a five-photon absorption process. Given the 2.1-eV energy of each 575-nm photon, this is a reasonable number of photons to be absorbed if the ionization threshold of THF is $\sim$8.5 eV, somewhat higher but still in line with our earlier estimate of $\sim$7.6 eV. At higher pump intensities, the slope of the curve changes to $\leqslant$1, showing that the initial five-photon process has been driven into saturation: Light at this intensity drives a 5+1 photon absorption process. The data for excitation at 500 nm (2.5 eV) are similar, except that the initial slope at low intensities is 4, also consistent with our expectations of an $\sim$8.5-eV ionization threshold for neat THF. For 395-nm (3.1 eV) excitation, the data show only a slope $\leqslant$1, indicating that the absorption process was driven into saturation at all intensities explored in the experiment.

Armed with the data in Fig. 3, we can now construct a consistent picture that explains the data in Figs. 1 and 2. The sensitivity of our pump-probe spectrometer limits how low we can go in pump intensity and still observe a transient signal. Thus, the pump-probe data presented in Figs. 1 and 2 were taken using pump intensities corresponding to the higher-intensity regime in Fig. 3. In combination with the observed linear signal dependence and the intensity-independent dynamics, we can conclude that our pump-probe experiments use more than the minimum required number of photons to ionize THF: We are likely using a 3+1 photoionization at 395 nm, doing a 4+1 photon process at 500 nm, and driving a 5+1 photon process at 575 nm. This means that for all three excitation wavelengths, we are providing $\sim$12.5 eV of total energy, or roughly 4 eV of excess energy to the photoejected electrons. This explains why all three transients are so similar, and also explains why the recombination decays are so slow: With such a large amount of excess energy, the thermalization length is expected to be quite large.

We can determine the thermalization lengths for the data in Fig. 2 by fitting the observed recombination decays to a standard model[7,50]

$$\Omega(t) = 1 - W_\infty W^*(t), \tag{1}$$

where $\Omega(t)$ is the survival probability for the ejected solvated electron, and

$$W_\infty = (1-\exp(-r_c/r_0))/[1-\exp(-r_c/R) \times [1-r_c D/vR^2]],$$

$$W^*(t) = \mathrm{erfc}(B) - \exp(A^2+2AB)\,\mathrm{erfc}(A+B),$$

$$A = (4R^2C/r_c^2)\sqrt{t/D}\,\sinh^2(-r_c/2R), \tag{2}$$

$$B = r_c(\coth(-r_c/2R) - \coth(-r_c/2r_0))/(4\sqrt{Dt}),$$

$$C = v - r_c D/[R^2(1-\exp(r_c/R))],$$

where r_c is the Onsager radius (the distance where the Coulomb energy equals the thermal energy, which for THF at room temperature with a dielectric constant $\epsilon = 7.5$ (Ref. 51) is 72 Å), D is the mutual diffusion constant of the recombining species, v is the reaction velocity (related to the bimolecular rate constant) and $\mathrm{erfc}(x)$ is the complementary error function. The model represented by Eqs. (1) and (2) assumes that the ejected electrons thermalize at a single distance r_0 from their parents (delta-function distribution), that both the electron and cation undergo diffusive motion in the presence of their mutual Coulomb attraction, and that the partners recombine instantly when the distance between them becomes less than the reaction radius R. To fit Eq. (1) to the data in Fig. 2, we used the known value of the electron diffusion constant in THF of 7.6×10^{-5} cm^2/s,[52] and assumed that the diffusion constant of the cation is small relative to that of the solvated electron. This leaves the thermalization length r_0, the reaction radius R and the reaction velocity v as the only adjustable parameters. The solid curves in Fig. 2 are fits of Eqs. (1) and (2) to the data. The fitted values of $R = 11\pm1$ Å and $v = 1.2\pm0.2$ m/s were forced to be identical for all three excitation wavelengths; the fitted thermalization lengths r_0 were found to be 46, 42, and 41 ± 3 Å for 395-, 500-, and 575-nm excitation, respectively.

The fitting parameters so obtained allow for the construction of a convincing physical picture of the microscopic dynamics. The large reaction distance of 11 Å, about twice the value of $\sim$5 Å seen in aqueous systems for the hydrated electron/OH radical pair,[16] is reasonable considering the larger radius of the solvated electron in THF than in water. The very large thermalization distances ($r_0 = 40$ Å) are consistent with the $\sim$4 eV of excess energy imparted to the electron by the 4-, 5-, or 6-photon absorption process for 395-, 500-, and 575-nm excitation, respectively. Finally, the reaction velocity of $\sim$1 m/s is of the same order of magnitude of the known value of $\sim$4 m/s for the hydrated electron/OH radical pair.[16] From these values we can conclude that the recombination dynamics of solvated electrons with their THF radical cation partners is governed by two competing factors: The large size of the solvated electron in THF, which would make recombination facile for electrons near their geminate cations (large R), and the very large amount of excess energy deposited by the multiphoton ionization event, which causes the majority of the electrons to thermalize far away so that recombination takes a long time (large r_0).

B. Electron production by CTTS excitation of sodide in THF

In this section, we use femtosecond pump-probe spectroscopy to monitor the dynamics of solvated electrons produced following CTTS excitation of Na^- in THF. The CTTS process is a unique way to generate solvated electrons in that it represents the simplest possible electron transfer reaction: The reactants and products have only electronic degrees of freedom, with the solvent behaving as both the promoter and the acceptor for charge transfer. Thus, the CTTS detachment of Na^- not only provides an alternate method than multiphoton ionization for generating solvated electrons in weakly polar fluids, but it also provides an ideal model system for studies of electron transfer.

In our previous paper, we found that following excitation of the CTTS band of Na^- in THF, solvated electrons were produced in ~700 fs, the time it takes for solvent motions to cause the electron to be ejected from the initially prepared localized excited state.[32] The dynamics of the solvated electron signal were independent of probe wavelength, suggesting that dynamic solvation does not play an important role in the spectroscopy of the newly formed equilibrium solvated electron. Instead, the transient absorption signals near 2 μm directly reflect the population of solvated electrons, so that the rise and fall of the signals correspond directly to the production and recombination of solvated electrons. We also found that the CTTS excited state (Na^-*) has a strong absorption near 590 nm, enabling us to monitor the ~700-fs decay of this state due to charge transfer. The neutral sodium atom product (Na^0) has a broad absorption which peaks near 880 nm;[53] by probing at 1150 nm, we were able to observe the appearance and disappearance of this species without interference from the Na^- ground state bleach or the absorption of the solvated electron.[32]

The observed pump probe transients in our previous paper could be fit well to a simple kinetic model, which we referred to as the ''delayed ejection'' model,[32]

$$Na^- \xrightarrow{h\upsilon} Na^-*, \tag{3}$$

$$Na^-* \underset{k_1}{\overset{\text{CTTS}}{\rightarrow}} Na^0 \cdot e^-_{\text{solvated}}, \tag{4}$$

$$Na^0 \bullet e^-_{\text{solvated}} \underset{k_2}{\overset{\text{recombination}}{\rightarrow}} Na^-, \tag{5}$$

$$Na^0 \bullet e^-_{\text{solvated}} \underset{k_3}{\overset{\text{escape}}{\rightarrow}} Na^0 + e^-_{\text{solvated}}. \tag{6}$$

Since the absorption spectra of Na^-, Na^0, and e^-_{solvated} are known, the model has only a few adjustable parameters, which are the absorption spectrum of Na^-* and the constants k_1, k_2, and k_3. Equation (3) represents the photoexcitation, which produces a bleach of the Na^- ground state and generates the ~590-nm absorbing Na^-* CTTS excited state. Equation (4) shows that the CTTS excited state then undergoes charge transfer with time constant $1/k_1 \approx 700$ fs, leading to the delayed appearance of both the solvated electron absorption, which can be probed near 2 μm, and the Na^0 absorption, which can be probed cleanly near 1150 nm. The $Na^0 \bullet e^-_{\text{solvated}}$ contact pair[54] can then undergo pseudo-first-order recombination with time constant $1/k_2 \approx 1.5$ ps, or the pair can separate, so that only a fraction $f = k_2/(k_2 + k_3)$ of the electrons undergo recombination, as described by Eqs. (5) and (6). For the ~500-nm pump wavelength we employed in our previous study, only a fraction $f \approx 0.4$ of the electrons undergo recombination with their sodium atom partners in the first few picoseconds following photoexcitation.[32]

Although the delayed ejection model fits the observed pump-probe transients remarkably well, it is oversimplistic in that it assumes that the spectra of all the species involved are static. Thus, the minor discrepancies between the fits to the model and the experimental data can be explained either by solvation dynamics that shift the absorption spectrum of the Na^0 product or by spectral diffusion in the ground state bleach. Recent experiments by Ruhman and co-workers have shown evidence for polarized hole-burning in the Na^-/THF system, suggesting that the ground state absorption band is inhomogeneously broadened.[55] Based on analogy with the electronically similar hydrated electron,[56] however, we do not believe that spectral diffusion in the ground state bleach is important for any of the magic angle (effectively unpolarized) pump-probe scans presented here or in our previous paper.[32] Thus, we believe that the delayed ejection model captures the correct ''zeroth order'' picture of the CTTS process, with the caveat that solvation dynamics on time scales faster than our instrument response undoubtedly lead to spectral shifts of the transient species that are not accounted for in our model.[55]

One question we did not address in detail in our previous paper is how the electron production and recombination dynamics vary as the excitation wavelength is tuned through the CTTS absorption band. Figure 4 presents the results of experiments monitoring the ~2-μm absorption of the THF-solvated electron following excitation at several different wavelengths: 395 (thin solid curve), 500 (dashed curve), 575 (dotted curve), and 640 nm (heavy solid curve). The upper panel shows the dynamics in the first 8 ps, with the transients normalized to have the same maximum change in absorbance; the lower panel shows the same data on a much longer time scale, with the transients normalized to the same change in absorbance at 8-ps delay. The short-time scans in the upper panel fit well to the delayed ejection model (fits not shown for clarity): The rates k_1 and k_2 do not change significantly with excitation, while the fraction f of electrons that recombine increases continuously as the excitation is tuned to the red, from $\leqslant$30% with 395-nm excitation to $\geqslant$95% with 800-nm excitation (data shown below in Fig. 5).

The invariance of the electron detachment rate k_1 with excitation wavelength[57] tells us quite a bit about the CTTS process. The rough constancy of k_1 is consistent with the basic picture of CTTS excitation being to a localized state. Increasing the excitation energy likely increases the spatial extent of the localized excited-state wave function, causing it to sample regions of the fluid farther from the Na atom core. Despite this extra delocalization, however, the same large-amplitude solvent motions are still required for the electron

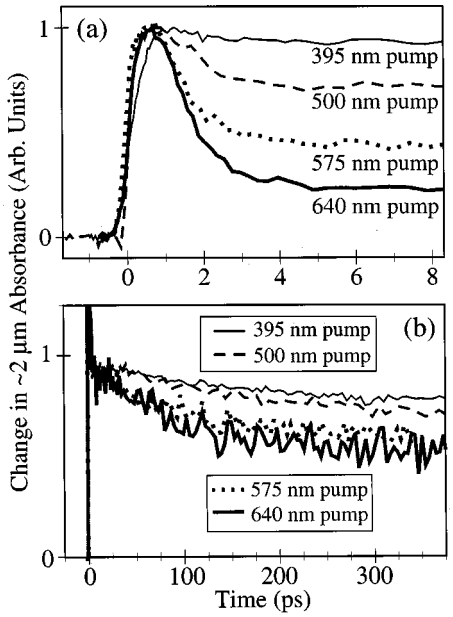

FIG. 4. Dynamics of the solvated electron's absorption at 2 μm following femtosecond excitation of Na^- in THF at a variety of pump wavelengths: 395 (thin solid curves), 500 (dashed curves), 575 (dotted curves) and 640 nm (heavy solid curves). (a) Short-time dynamics with transients normalized to the same maximum change in absorbance. (b) Dynamics on a longer time scale with transients normalized to have the same change in absorbance at a time delay of 8 ps.

to detach, so that the CTTS charge transfer is rate-limited by this motion of the solvent. This is in sharp contrast to the results of the previous section, where electrons are ejected directly into the solvent by multiphoton ionization so that there is a direct correlation between the excitation energy and thermalization length. This idea of the CTTS electron detachment rate being roughly independent of excitation energy is consistent with the results of recent MD simulations: The rate limiting step in solvating the species involved in charge transfer reactions involves the translational motions of solvent molecules that accommodate the new size of the solute following detachment of the electron.[58]

The invariance of the recombination rate k_2, combined with the strong dependence of the recombination fraction f on excitation wavelength, provides insight into the nature of the contact pair formed following CTTS. The fact that all the pairs that recombine do so at the same rate while the number of recombining pairs changes with excitation wavelength suggests that two different species can be formed upon CTTS excitation. At low excitation energies, the CTTS excited-state wave function is strongly confined to the region near the sodium nucleus; the resulting solvent motions cannot transport the electron far away from the parent. Since the solvated electron in THF is a highly delocalized object, there is a strong probability that the detached electron's wave function will overlap with that of its geminate sodium atom partner. This overlap leads to a large probability for direct non-adiabatic recombination, which occurs on the observed $\sim$1.5-ps time scale.[32] At higher excitation energies, the CTTS excited-state wave function is more delocalized, so there is an increased probability that solvent motions will cause the electron to detach and localize in regions a bit farther out into the fluid. For those electrons that still localize close in, recombination still occurs in $\sim$1.5 ps. For those electrons that localize just a little bit farther out, the overlap goes to zero, leading to essentially no probability for direct nonadiabatic recombination. As the excitation energy is increased, a higher fraction of the detached electrons will have no overlap with the nearby Na atom, leading to a lower probability for recombination. Thus, Fig. 4(a) provides evidence for two different types of electrons ejected during the CTTS process: those that localize nearby so that they overlap with their geminate partner, and those that localize far enough away so that overlap with their geminate partner is negligible.

The next logical question to ask is what is the fate of the electrons that are ejected far enough from the Na atom that they do not recombine in the first few ps? Figure 4(b) explores the dynamics of the detached solvated electrons for several hundred picoseconds after CTTS detachment. The electrons that survive the first few ps undergo recombination on a time scale similar to that observed for multiphoton ionization of the neat solvent, as seen in the previous section. If the early recombination dynamics is ignored, we can attempt to fit the long-time tails of the transients shown in Fig. 4(b) to a standard recombination model that assumes a Gaussian distribution of thermalization distances followed by diffusive recombination,[59]

$$\Omega(t) = \mathrm{erfc}(R/\sqrt{4Dt_g}) + [R \cdot \exp(-R^2/4D(t+t_g))/ \sqrt{\pi \cdot D(t+t_g)}] \cdot \mathrm{erfc}(\sqrt{R^2 t/4Dt_g(t+t_g)}), \quad (7)$$

where $\Omega(t)$ is the survival probability of the electron, R is the reaction distance, $t_g = \sigma^2/2D$, D is the mutual diffusion constant (which we assume to be equal to the diffusion constant of the electron), σ is the width of the Gaussian distribution of thermalization distances (giving $\langle r_0 \rangle = (8/\pi)^{1/2}\sigma$ as the average thermalization distance of the Gaussian distribution). The model represented by Eq. (7) differs from that in Eqs. (1) and (2) in that there is no Coulomb potential acting between the recombining species (since the Na atom partner is neutral) and that there is a Gaussian distribution of initial distances rather than a single initial thermalization distance. The quality of the fits (not shown), especially the high signal-to-noise scan with 395-nm excitation, is poorer than that seen in Fig. 2: The functional form represented by Eq. (7) has the wrong curvature to perfectly describe the data. If the model is employed anyway, the best fit parameters of Eq. (7) to the data in Fig. 4(b) result in a value of 45 ± 3 Å for the reaction distance R, and in values of the average thermalization distance $\langle r_0 \rangle$ of 55, 61, 73, and 83 ± 5 Å for excitation at 640, 575, 500, and 395 nm, respectively.

In addition to the poor functional form, the values of the reaction and thermalization distances obtained by fitting the data in Fig. 4(b) to Eq. (7) are physically unreasonable. First, the reaction distance R of $\sim$45 Å is exceedingly large; even with the highly delocalized wave function of the solvated electron in THF, there is no way that the electron could tunnel through several intervening solvent shells to recombine instantaneously with its geminate Na atom partner from a distance of $\sim$45 Å. Second, the average thermalization

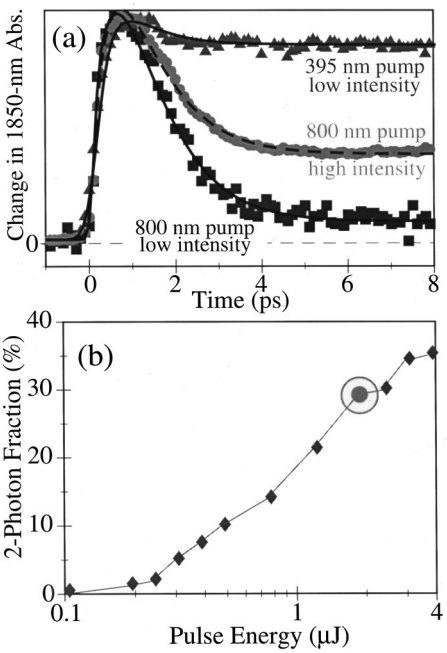

FIG. 5. (a) Dynamics of the solvated electron's absorption probed at 1850 nm following femtosecond excitation of Na^- in THF at 800 nm with low intensity (squares), 395 nm with low intensity (triangles), and at 800 nm with high intensity (circles). The fit to the high-intensity data (thin dashed line) is a linear combination of the fits to the low-intensity data (thin solid lines); see text for details. (b) Fraction of the fit to the high-intensity data (two-photon contribution) as a function of pump intensity. The circled point near 2 μJ excitation intensity with ~30% two-photon contribution corresponds to the high-intensity data shown in Fig. 5(a). The lines connect the data points and are drawn to guide the eye.

distances $\langle r_0 \rangle$, which exceed 80 Å, are much larger than thermalization lengths obtained for the multiphoton ionization of the neat solvent discussed above. An ~80 Å thermalization distance following the one-photon CTTS detachment makes little sense since the total photon energy involved is only a few eV: It is unlikely that there is enough excess energy available to eject electrons to distances this large (cf. the ~40 Å ejection distance with ~4 eV of excess energy for the multiphoton ionization in the previous section). Moreover, we know from Fig. 4(a) that a significant fraction of the ejected electrons thermalize close enough to their partner Na atoms to form overlapping contact pairs and undergo recombination in <2 ps. It is difficult to imagine a mechanism that causes some ejected electrons to remain close to their partners in an overlapping contact pair while the remaining electrons are ejected up to 80 Å away. Thus, the only conclusion that can be drawn from the fits to the data in Fig. 4(b) is that a diffusive process is not the best description of the recombination seen at long times following CTTS detachment.

The fact that simple diffusion models like Eq. (7) cannot adequately describe the data in Fig. 4(b) leads us to propose an alternate picture to explain the long-time recombination following CTTS. Following CTTS excitation, solvent motions cause the electron to detach and solvate nearby the geminate Na atom. At low excitation energies, the electron ejection distance is likely to be on the order of 3 to 4 Å; since the radius of the solvated electron in THF is ~3.4 Å,[42] there is enough overlap to lead to direct nonadiabatic recombination on the ~1.5-ps time scale. At higher excitation energies, the electron can be ejected just far enough away so that there is an intervening solvent molecule between the electron and the Na atom, forming a solvent-separated contact pair that has negligible wave function overlap. We believe that the $Na^0/e^-_{solvated}$ solvent-separated contact pair has behavior similar to that seen following ionization of indole: Even though recombination is energetically favorable, there is a large free energy barrier to break up the solvent structure around the separated contact pair, inhibiting the back electron transfer.[23] In other words, the back electron transfer from the solvent-separated contact pair can be thought of as occurring in the Marcus inverted regime. The small wavelength dependence to the long-time decays in Fig. 4(b) is consistent with this idea. Higher energy excitation produces contact pairs with a slightly higher degree of separation and thus a higher barrier for back electron transfer, leading to the observed slightly slower recombination dynamics. Overall, the best basic description of the CTTS process is that of the delayed ejection model with one modification: Electrons that do not undergo the direct recombination process of Eq. (5) end up in solvent-separated contact pairs, which can undergo thermally activated recombination on a time scale of hundreds of ps.

One question that remains is whether the distance that electrons are ejected during the CTTS process depends only on the amount of excess energy deposited. It is certainly possible that the featureless CTTS band of Na^- is comprised of multiple overlapping transitions. This leads to the possibility that as the excitation wavelength is changed, a different fraction of each transition is being excited, causing electrons to be ejected at different distances. To investigate this possibility, we performed intensity-dependent pump-probe experiments on Na^-, the results of which are shown in Fig. 5. The squares in Fig. 5(a) show the change in absorption at 2 μm following low-intensity excitation at 800 nm. These photons have a low enough energy to ensure that nearly all the ejected electrons thermalize close enough to their geminate partners to recombine directly in $\leqslant 2$ ps. The triangles in Fig. 5(a) show similar low-intensity data taken using 395-nm excitation. The solid lines through these two sets of data in Fig. 5(a) are multiexponential fits to the data. The circles show the results of an experiment monitoring the solvated electron absorption following high-intensity excitation at 800 nm. It is clear that at high excitation intensity, the relative weight of fast geminate recombination with the Na atom partner decreases. This is undoubtedly a signature of two-photon absorption becoming important at high pump fluences.

We can describe the effects of this two-photon absorption at high intensities in a straightforward way. The dashed line through the high-intensity transient in Fig. 5(a) is a fit to a linear combination of the fits to the low-intensity data for both 800- and 395-nm excitation [solid lines in Fig. 5(a)]. We performed similar experiments at a variety of excitation intensities, and in every case the simple linear combination fits the data remarkably well. Figure 5(b) summarizes the results of these experiments, plotting the fraction of the two-

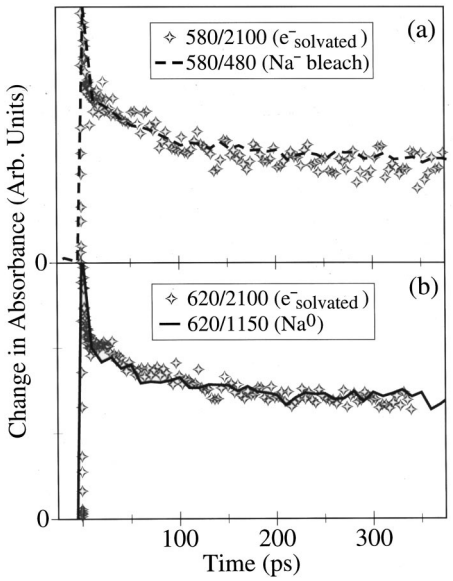

FIG. 6. Femtosecond transient absorption traces of the important kinetic species in the CTTS excitation of Na^- in THF. (a) Following 580-nm excitation, the open diamonds show the dynamics of the solvated electron at 2100 nm; the dashed curve monitors the (negative of the) ground state bleach of the parent Na^- at 480 nm. (b) Following 620-nm excitation, the open diamonds show the dynamics of the solvated electron at 2100 nm; the solid curve monitors the absorption of Na^0 at 1150 nm.

photon component of the fit (i.e., the fraction of the linear combination coming from the fit to the 395-nm data) as a function of excitation intensity. At low intensities the CTTS excitation is clearly in the one-photon regime, but at higher intensities above a few hundred nJ/pulse (with a $\sim$300-μm diameter spot size), two-photon excitation is becoming increasingly important. By using the data in Fig. 5(b) and the expected intensity-squared dependence for two-photon absorption, we can determine the two-photon absorption cross section of Na^- at 800 nm to be $\sim 10^{10}$ cm^4/(J mol), a surprisingly large value. We emphasize that with the exception of the circles in Fig. 5(a), all the pump-probe transients on Na^- shown in this paper were taken with pump pulse energies below 200 nJ, safely out of the regime where two-photon absorption is important. Overall, the results in Fig. 5(b) lead us to conclude that two-photon excitation at 800 nm produces the same recombination dynamics as single-photon excitation at 395 nm: The electron ejection distance depends only on the excitation energy, and not on whether it is provided by one 395- or two 800-nm photons.

We close this section by verifying that the conclusions we have drawn by measuring the dynamics of the solvated electron near 2 μm also hold when investigating the other species involved in the CTTS process. We know from our previous work that the bleach of the Na^- ground state can be detected most cleanly to the blue of 500 nm, where neither the Na^-* excited state nor the Na^0 product strongly absorb.[32] Figure 6(a) compares the recombination dynamics of the solvated electron (open diamonds) to the bleach recovery of the Na^- ground state (dashed curve). The two transients clearly agree within the signal-to-noise, showing that the same recombination events that decrease the absorbance of solvated electrons cause the bleach of the ground state to recover, indicating that recombination leads to reformation of ground-state Na^-. Figure 6(b) makes a similar comparison between the dynamics of the solvated electron (open diamonds) and that of the neutral sodium atom product probed at 1150 nm (solid curve). As expected, the transients are in excellent agreement, supporting the idea that the ejected electrons combine only with Na atoms and not with any scavengers that might be present in solution. Overall, the data in Fig. 6 verify that our basic picture of both the spectroscopy and the dynamics of the Na^- system is fundamentally correct.[32]

IV. DISCUSSION

In this paper, we have explored the mechanisms of electron production and recombination in THF both for multiphoton ionization of the neat solvent and for electron detachment via the CTTS transition of Na^-. The recombination of solvated electrons produced via multiphoton ionization of neat THF can be well described by a simple diffusive model. The recombination of solvated electrons ejected via CTTS detachment of Na^-, on the other hand, takes place on two distinct time scales of $\leqslant$2 and $\sim$200 ps with kinetics that cannot be adequately fit by simple diffusive models, leading us to postulate the presence of both directly overlapping and solvent-separated Na atom:solvated electron contact pairs to explain the observed dynamics. The dramatic differences in recombination remind us that the electron generation mechanisms are fundamentally different for the two processes. Multiphoton ionization causes ejection of electrons into the equilibrium structure of the fluid. Since the fluid is isotropic, the only preference the electron has for localizing either close to or far from its parent is determined by the amount of excess energy provided during the ionization process. Excitation of the CTTS band, in contrast, results in an electron transfer reaction. The electrostatic interaction between the electron and the parent nucleus is not sufficient to bind the CTTS excited state; the favorable interactions between the electron and the local solvent structure established by the parent anion are also required. Photoexcitation disrupts the local solvent environment, which leads to ejection of the excited electron. The solvent motions that lead to ejection, however, must stabilize *both* the neutral atom and the solvated electron, leading to formation of a stable neutral atom: solvated electron contact pair. Thus, the differences in the two processes serve to emphasize that CTTS is an inherently local phenomenon controlled by the details of solvent motions in the immediate vicinity of the parent ion, while multiphoton ionization produces a delocalized electron whose wave function is largely unaffected by the solvent before undergoing localization.

For the case of multiphoton ionization of neat THF, we found it difficult to eject electrons at energies just above the ionization threshold. At all three excitation wavelengths we selected, the ejection process used one more photon than that minimally required to ionize the solvent. This leads us to conclude that there is a broad continuum of excited states in the THF molecule near the ionization threshold of $\sim$8.5 eV, providing intermediate levels that resonantly enhance the absorption of the last photon in the multiphoton ionization pro-

cess. As a result, when the different numbers of photons absorbed are accounted for, the multiphoton absorption process at all the excitation wavelengths we selected for this study provided about 12.5 eV of energy, leaving ~4 eV of excess energy for the ejected electrons. Fits to a standard diffusion model suggest that the ejected electrons localize ≥40 Å from their cation partners, and can recombine when they diffuse to within ~10 Å. In a similar study on liquid water, Crowell and Bartels found that with ~4 eV of energy above the ionization threshold, the mean thermalization distance of the ejected electron was ~35 Å with a reaction distance of ~5 Å.[15] The fact that the reaction distance in THF is twice that in water is consistent with the fact that the spatial extent of the solvated electron in THF is nearly double that of the hydrated electron. The thermalization distance in THF is comparable to that seen in water, indicating that excess energy plays a similar role in the electron ejection process in both fluids.

The large thermalization distances we observe for electrons ejected via multiphoton ionization of THF preclude the possibility of rapid geminate recombination, as had been assigned in previous studies of multiphoton ionization of nonpolar fluids.[9] The fast absorption decays we observe in the visible region of the spectrum do not match the kinetics measured for the solvated electron at ~2 μm, and therefore cannot be assigned to geminate recombination. While dynamic solvation or vibrational cooling could explain the observed absorption changes in the visible, it is unlikely that either of these processes would lead to the observed order of magnitude decrease in absorbance at 575 nm. Instead, we believe the most likely explanation of the visible absorption dynamics is a chemical reaction involving the THF radical cation, possibly a hydrogen-atom abstraction reaction with a nearby THF molecule. The data we have presented do not rule out the possibility that fast geminate recombination could occur in THF or similar fluids if the ionization were near threshold, but the only unambiguous signature of this would be a rapid decay of the solvated electron's characteristic infrared absorption.

For the CTTS transition of Na^-, excitation of one of the outermost electrons in the Na 3*s* orbital produces a localized, *p*-like excited state. The electronic wave function of this distorted *p* state samples only the nearby fluid, so the solvent motions that ultimately lead to charge transfer after ~700 fs can expel the electron only into a nearby cavity, just a few angstroms away. If the ejected electron's wave function overlaps its geminate Na atom partner, direct nonadiabatic recombination occurs within 2 ps. At higher excitation energies, the excited state wave function can sample regions farther into the liquid, leading to the possibility of ejection far enough away to form a solvent-separated contact pair. In this latter case, the process of breaking up the solvent structure around both the Na atom and the solvated electron creates a large free energy barrier to recombination, so that the back electron transfer occurs on a time scale of hundreds of picoseconds. The distance the electron is ejected from the CTTS excited state correlates only with excess energy; it does not matter, for example, whether the excitation uses one 395-nm photon or two 800-nm photons.

The idea of producing a stable contact pair following detachment of an electron from a solute[30] has also been invoked in related experiments on aqueous systems. Bradforth and co-workers noted that following CTTS detachment from aqueous iodide, geminate recombination takes place on a tens of picoseconds time scale.[28] The recombination decays did not fit to standard diffusive models; like what we saw for the long-time recombination in the Na^- system, the fits to the iodide data produced reaction distances and thermalization lengths that were unphysically large. Thus, Bradforth and co-workers concluded that the electrons ejected from CTTS excitation of iodide do not recombine diffusively and are instead localized close by in a contact pair.[28] In the photoionization of indole in water, Kohler and co-workers noted that following electron detachment there was essentially no geminate recombination.[23] Since the excitation energy in their experiments was expected to be just above the ionization threshold, these workers concluded that the ejected electrons were localized in a contact pair with a barrier for recombination that is large compared to kT at room temperature.[23] Overall, the results of all these related experiments suggest that for the localized excitation of a solute, the solvent motions that solvate the photoionized parent species and lead to electron detachment intrinsically tend to produce stable solvated electron:geminate partner contact pairs.

The relative rates at which recombination occurs in these different examples of electron detachment can be rationalized by considering the structure of the solvated electron in different environments. In the iodide CTTS system, the compact form of the hydrated electron makes it unlikely that there will be any direct overlap of the detached electron's wave function with its geminate iodine atom partner. This explains why the direct recombination observed on the ~2-ps time scale in the Na^-/THF system is absent in the case of aqueous iodide. Once the electron is ejected from iodide, half of the stability of the contact pair involves the hydrophobic hydration of the nonpolar iodine atom. Since solvation of a nonpolar species in water is energetically unfavorable, the barrier for breaking up the solvent structure around the iodine atom to initiate recombination of the contact pair is small, so recombination proceeds within tens of ps.[28] For the Na^- system, the nonpolar Na atom should be quite favorably solvated by the weakly polar THF solvent. This means there is a somewhat larger barrier to break up the solvent-stabilized contact pair in the Na^- system than in the iodide system, leading to the observed recombination dynamics on the hundreds of picoseconds time scale. Finally, in the indole work of Kohler and co-workers, the contact pair consists of an indole radical cation adjacent to the hydrated electron. The barrier to break up the solvent structure around two ions in water is expected to be quite large, so that essentially no recombination can take place at room temperature.[23]

The contact pairs in all these systems consist of a solvated electron separated by (at least) one solvent molecule from its solvated geminate partner. This makes it very unlikely that the electron and its geminate partner interact strongly enough to cause a significant perturbation in the electronic structure of either species. In other words, we expect that the absorption spectrum of the contact pair is at

most only subtly different from the sum of the absorption spectra of the isolated partner and solvated electron. In the previous aqueous work on both iodide[28] and indole,[23] the measured spectrum of the hydrated electron in the contact pair was identical within the experimental accuracy to the spectrum of an isolated hydrated electron. The delayed ejection model we used to describe the kinetics of the Na^- system provided an excellent fit to the data assuming that the spectrum of the contact pair is simply the sum of the spectra of the equilibrium neutral sodium atom and the solvated electron.[54] This view of solute-electron contact pairs as a kinetically important but not spectroscopically distinct species differs from that proposed elsewhere in the literature: Experiments that excited the CTTS transition of aqueous halides by multiphoton ionization claim to have found kinetic evidence for several spectroscopically distinct contact pairs.[26] The multiphoton excitation used in these other experiments, however, is more akin to multiphoton ionization of the solvent and thus is not likely to produce stable contact pairs, spectroscopically distinct or otherwise. The place where we anticipate that the proximity of the electron and its geminate partner will have the biggest spectroscopic effect is in the localization dynamics of the ejected electron. The solvent relaxation around the electron in a contact pair is quite likely to be different from that of a free solvated electron. This type of phenomenon is difficult to see in weakly polar fluids like THF where the broad, featureless spectrum of the solvated electron results in identical kinetic traces throughout the absorption band. In aqueous systems, however, it might be possible to distinguish the formation dynamics of a free hydrated electron from that of an electron localizing in a contact pair.[28]

Finally, the time scale of the fast geminate recombination in the Na^-/THF system allows us to speculate on the nature of the Na^0 species. It is not immediately clear if this species is better identified as a solvated neutral sodium atom or a solvated electron:sodium cation contact pair (the difference being whether or not the center of mass of the electron coincides with the sodium nucleus or with an adjacent cavity in the solvent).[53] The presence of the direct recombination channel on the $\sim$1.5-ps time scale argues that a solvated neutral atom is likely the better description. Figure 6 makes it clear that recombination produces an immediate loss of the Na^0 signal and an immediate recovery of the ground state bleach. If the partner species consisted of a separated sodium cation and solvated electron, then recombination to re-form the Na^- parent ground state would require a three-body event: Both electrons would have to recombine simultaneously with the sodium cation. Since this type of recombination is unlikely (although not impossible), and since the spectrum of the Na^0 species does not appear to change with time, we believe that this entity is best described as a solvated neutral sodium atom.

ACKNOWLEDGMENTS

This work was supported by a National Science Foundation CAREER Award (Grant. No. CHE-9733218). Benjamin J. Schwartz is a Cottrell Scholar of Research Corporation and an Alfred P. Sloan Foundation Research Fellow. We thank Steve Bradforth for many stimulating discussions related to this work, and Rob Crowell for suggesting the nonlinear absorbance experiment and providing a preprint of Ref. 39.

[1] See, e.g., J. M. Warman, *The Study of Fast Processes and Transient Species by Electron Pulse Radiolysis*, edited by J. H. Baxendale and F. Bus (Reidel, Dordrecht, 1983), p. 433; B. C. Le Motais and C. D. Jonah, Radiat. Phys. Chem. **33**, 505 (1989), and references therein.
[2] See, e.g., J. T. Hynes, in *Ultrafast Dynamics of Chemical Systems*, edited by J. D. Simon (Kluwer Academic, Netherlands, 1994), Ch. 13, p. 345; P. F. Barbara, T. J. Meyer, and M. A. Ratner, J. Phys. Chem. **100**, 13148 (1996).
[3] P. J. Rossky and J. D. Simon, Nature (London) **370**, 263 (1994); P. J. Rossky, J. Opt. Soc. Am. B **7**, 1727 (1990).
[4] F. H. Long, H. Lu, X. Shi, and K. B. Eisenthal, Chem. Phys. Lett. **185**, 47 (1991); F. H. Long, H. Lu, and K. B. Eisenthal, *ibid.* **160**, 464 (1989); Phys. Rev. Lett. **64**, 1469 (1990); H. Lu, F. Long, R. Bowman, and K. B. Eisenthal, J. Chem. Phys. **93**, 27 (1989).
[5] Y. Gauduel, S. Pommeret, and A. Antonetti, J. Phys. I **1**, 127 (1991); S. Pommeret, A. Antonetti, and Y. Gauduel, J. Am. Chem. Soc. **113**, 9105 (1991); A. Migus, Y. Gauduel, J. L. Martin, and A. Antonetti, Phys. Rev. Lett. **58**, 1559 (1987); Y. Gauduel, S. Pommeret, A. Migus, and A. Antonetti, Chem. Phys. Lett. **149**, 1 (1990).
[6] R. Laenen, T. Roth, and A. Laubereau, Phys. Rev. Lett. **85**, 50 (2000); A. Hertwig, H. Hippler, A. N. Unterreiner, and P. Vöhringer, Ber. Bunsenges. Phys. Chem. **102**, 805 (1998); J. L. McGowen, H. M. Ajo, J. Z. Zhang, and B. J. Schwartz, Chem. Phys. Lett. **231**, 504 (1994).
[7] C. L. Thomsen, D. Madsen, S. R. Keiding, and J. Thøgersen, J. Chem. Phys. **110**, 3453 (1999).
[8] C. Pepin, D. Houde, H. Remita, T. Goulet, and J.-P. Gerin, Phys. Rev. Lett. **69**, 3389 (1992); J. Phys. Chem. A **101**, 4351 (1997).
[9] F. H. Long, H. Lu, and K. B. Eisenthal, J. Phys. Chem. **99**, 7436 (1995); H. Lu, F. H. Long, and K. B. Eisenthal, J. Opt. Soc. Am. B **7**, 1511 (1990); R. M. Bowman, H. Lu, and K. B. Eisenthal, J. Chem. Phys. **89**, 606 (1988).
[10] M. U. Sander, U. Brummund, K. Luther, and J. Troe, J. Phys. Chem. **97**, 8378 (1993); Ber. Bunsenges. Phys. Chem. **96**, 1486 (1992).
[11] Y. Hirata and N. Mataga, J. Phys. Chem. **95**, 1640 (1991); *ibid.* **93**, 7539 (1989); N. Mataga, Radiat. Phys. Chem. **32**, 177 (1988).
[12] E. Keszei, T. H. Murphrey, and P. J. Rossky, J. Phys. Chem. **99**, 22 (1995); T. H. Murphrey and P. J. Rossky, J. Chem. Phys. **99**, 515 (1993); F. A. Webster, J. Schnitker, M. S. Friedrichs, R. A. Friesner, and P. J. Rossky, Phys. Rev. Lett. **66**, 3172 (1991).
[13] S. M. Pimblott and J. A. LaVerne, J. Phys. Chem. A **102**, 2967 (1998); S. M. Pimblott, J. A. LaVerne, D. M. Bartels, and C. D. Jonah, J. Phys. Chem. **100**, 9412 (1996); S. M. Pimblott, J. A. LaVerne, A. Mozumder, and N. J. B. Green, *ibid.* **94**, 488 (1990).
[14] L. Onsager, J. Chem. Phys. **2**, 599 (1934); Phys. Rev. **54**, 554 (1938); K. M. Hong and J. Noolandi, J. Chem. Phys. **69**, 5026 (1978).
[15] R. A. Crowell and D. M. Bartels, J. Phys. Chem. **100**, 17940 (1996).
[16] T. Goulet and J.-P. Jay-Gerin, J. Chem. Phys. **96**, 5076 (1992); N. J. B. Green, M. J. Pilling, S. M. Pimblott, and P. Clifford, J. Phys. Chem. **94**, 251 (1990).
[17] See, e.g., H. T. Davis and R. G. Brown, Adv. Chem. Phys. **31**, 325 (1975).
[18] For simulations of electrons in nonpolar fluids, see, e.g., Z. Liu and B. Berne, J. Chem. Phys. **99**, 9054 (1993).
[19] L. M. Dorfman, F. Y. Jou, and R. Wageman, Ber. Bunsenges. Phys. Chem. **75**, 681 (1971); F. Y. Jou and G. R. Freeman, Can. J. Phys. **54**, 3693 (1976).
[20] J. W. Boag and E. J. Hart, Nature (London) **197**, 45 (1963); F.-Y. Jou and G. R. Freeman, J. Phys. Chem. **83**, 2383 (1979).
[21] J. C. Mialocq, J. Chim. Phys. Phys.-Chim. Biol. **85**, 31 (1988); N. Getoff, Radiat. Phys. Chem. **34**, 711 (1989).
[22] See, e.g., Y. Hirata, Y. Tanaka, and N. Mataga, Chem. Phys. Lett. **193**, 36 (1992), and references therein.
[23] J. Peon, G. C. Hess, J.-M. L. Pecourt, T. Yuzawa, and B. Kohler, J. Phys. Chem. A **103**, 2460 (1999).
[24] M. J. Blandamer and M. F. Fox, Chem. Rev. **70**, 59 (1970); J. Jortner, M. Ottolenghi, and G. Stein, J. Phys. Chem. **68**, 247 (1964); L. I. Grossweiner and M. S. Matheson, *ibid.* **61**, 1089 (1957); M. S. Matheson, W. A. Mulac, and J. Rabani, *ibid.* **67**, 261 (1963).
[25] F. H. Long and K. B. Eisenthal, J. Phys. Chem. **98**, 7252 (1994); F. H.

Long, H. Lu, X. Shi, and K. B. Eisenthal, Chem. Phys. Lett. **169**, 165 (1990); F. H. Long, H. Lu, and K. B. Eisenthal, J. Chem. Phys. **91**, 4413 (1989).
[26] H. Gelabert and Y. Gauduel, J. Phys. Chem. **100**, 13993 (1996); Y. Gauduel, H. Gelabert, and M. Ashokkumar, Chem. Phys. **197**, 167 (1995); Y. Gauduel, S. Pommeret, A. Migus, N. Yamada, and A. Antonetti, J. Opt. Soc. Am. B **7**, 1528 (1990).
[27] M. Assel, R. Laenen, and A. Laubereau, Chem. Phys. Lett. **289**, 267 (1998).
[28] J. A. Kloepfer, V. H. Vilchiz, V. A. Lenchenkov, and S. E. Bradforth, Chem. Phys. Lett. **298**, 120 (1998); J. A. Kloepfer, V. H. Vilchiz, V. A. Lenchenkov, A. C. Germaine, and S. E. Bradforth, J. Chem. Phys. **113**, 6288 (2000); V. H. Vilchiz, J. A. Kloepfer, A. C. Germaine, V. A. Lenchenkov, and S. E. Bradforth, J. Phys. Chem. (submitted).
[29] W.-S. Sheu and P. J. Rossky, J. Phys. Chem. **100**, 1295 (1996); J. Am. Chem. Soc. **115**, 7729 (1993); Chem. Phys. Lett. **213**, 233 (1993); **202**, 186 (1993).
[30] D. Borgis and A. Staib, J. Phys.: Condens. Matter **8**, 9389 (1996); J. Chem. Phys. **104**, 4776 (1996); A. Staib and D. Borgis, *ibid.* **104**, 9027 (1996); D. Borgis and A. Staib, Chem. Phys. Lett. **230**, 405 (1994).
[31] See, e.g., E. Neria and A. Nitzan, J. Chem. Phys. **99**, 1109 (1993); R. D. Coalson, D. G. Evans, and A. Nitzan, *ibid.* **101**, 436 (1994).
[32] E. R. Barthel, I. B. Martini, and B. J. Schwartz, J. Chem. Phys. **112**, 9433 (2000).
[33] J. L. Dye, Prog. Inorg. Chem. **32**, 327 (1984); J. Phys. IV **1**, 259 (1992); M. T. Lok, F. J. Tehan, and J. L. Dye, J. Phys. Chem. **76**, 2975 (1972).
[34] J. G. Kloosterboer, L. J. Giling, R. P. H. Rettschnick, and J. D. W. Van Voorst, Chem. Phys. Lett. **8**, 462 (1971); W. A. Seddon and J. W. Fletcher, J. Phys. Chem. **84**, 1104 (1980).
[35] I. Hurley, T. R. Tuttle, and S. Golden, J. Chem. Phys. **48**, 2818 (1968).
[36] J. L. Dye, J. Phys. Chem. **84**, 1084 (1980).
[37] J. L. Dye, J. Chem. Educ. **54**, 332 (1977); R. R. Dewald and K. W. Browall, J. Phys. Chem. **74**, 129 (1970); R. R. Dewald and J. L. Dye, *ibid.* **68**, 128 (1964).
[38] T.-Q. Nguyen, I. B. Martini, J. Liu, and B. J. Schwartz, J. Phys. Chem. B **104**, 237 (2000).
[39] R. A. Crowell and J. Qian (to be published).
[40] S. H. Lin, Y. Fujimura, H. J. Neusser and E. W. Schlag, *Multiphoton Spectroscopy of Molecules* (Academic, Orlando, 1984).
[41] I. Becker, G. Markovich, and O. Cheshnovsky, Phys. Rev. Lett. **79**, 3391 (1997); I. Becker and O. Cheshnovsky, J. Chem. Phys. **110**, 6288 (1999).
[42] L. Kevan, J. Phys. Chem. **84**, 1232 (1980).
[43] P. J. Rossky and J. Schnitker, J. Phys. Chem. **92**, 4277 (1988); J. Schnitker, K. Motakabbir, P. J. Rossky, and R. A. Friesner, Phys. Rev. Lett. **60**, 456 (1988).
[44] The Chemical Rubber Company, *Handbook of Chemistry and Physics*, 80th ed. (CRC, New York, 1999), Vol. 10, p. 188.
[45] Y. Heimlich, V. Rozenshtein, H. Levanon, and L. Lukin (to be published); V. Rozenshtein, Y. Heimlich, and H. Levanon, J. Phys. Chem. A **101**, 3197 (1997).
[46] We note that the first ~250 fs of the data are sometimes subject to a coherence artifact which is not reproducible at different probe wavelengths. Thus, there is a small possibility that the coherence artifact masks spectral evolution of the solvated electron's absorption spectrum on these very short time scales. Experiments with shorter pulses should be able to resolve this issue.
[47] M. A. Lewis and C. D. Jonah, Radiat. Phys. Chem. **33**, 1 (1989); J. H. Baxendale, C. Bell, and P. Wardman, J. Chem. Soc., Faraday Trans. 1 **69**, 776 (1973); P. Ausloos, R. E. Rebbert, F. P. Schwarz, and S. G. Lias, Radiat. Phys. Chem. **21**, 27 (1983); S. Tagawa, M. Washio, H. Kobayashi, Y. Katsamura, and Y. Tabata, *ibid.* **21**, 45 (1983); R. Mehnert, O. Brede, and W. Naumann, *ibid.* **26**, 499 (1985).
[48] We note that unlike the signal at 2 μm, which probes the solvated electron, the 575-nm transient shows a polarization dependence, suggesting that the visible-absorbing species undergoes rotational diffusion on a tens or hundreds of picoseconds time scale.
[49] The excitation intensities used for the pump-probe experiments in this study could be varied by only a factor of ~10 from ~1 to ~10 mJ/cm^2; lower intensities resulted in signals too small for effective signal averaging.
[50] N. J. B. Green, Chem. Phys. Lett. **107**, 485 (1984). We note that this model is strictly only applicable in high permittivity solvents. Our purpose in applying the model to our data in low-permittivity THF is only to obtain a semiquantitative estimate of the thermalization distances involved. The errors in using the high permittivity formula for our low permittivity situation should be large only at early times, and thus are expected to have only a minor systematic effect on the fitted values of r_0; see, e.g., P. Clifford, N. J. B. Green, and M. J. Pilling, J. Phys. Chem. **88**, 4171 (1984).
[51] The Chemical Rubber Company, *Handbook of Chemistry and Physics*, 80th ed. (CRC, New York, 1999), Vol. 6, p. 154.
[52] The diffusion constant of the solvated electron in THF was calculated by using the Einstein relation, $D=(kT/e)\mu$, where e is the elementary charge and μ is the mobility of the electron. See, e.g., Ref. 45 or S. M. Sze, *Physics and Properties of Semiconductor Devices*, 2nd ed. (Wiley, New York, 1981), p. 30; P. W. Atkins, *Physical Chemistry*, 5th ed. (W. H. Freeman, New York, 1994), p. 849. The mobility of the excess electron in THF has been reported as 3×10^{-3} cm^2/Vs: J.-P. Dodelet and G. R. Freeman, Can. J. Chem. **53**, 1263 (1975).
[53] P. Piotrowiak and J. R. Miller, J. Am. Chem. Soc. **113**, 5086 (1991); B. Bockrath and L. M. Dorfman, J. Phys. Chem. **79**, 1509 (1975); **77**, 1002 (1973).
[54] In the delayed ejection model, we assume that the $Na0^0 \bullet e^-_{solvated}$ contact pair has an absorption spectrum equal to the sum of that of the isolated Na^0 atom and the isolated $e^-_{solvated}$.
[55] Z. Wang, O. Shoshana, and S. Ruhman, Proceedings of the 12th International Conference on Ultrafast Phenomena [Springer-Verlag, New York (in press)]; Z. Wang, O. Shoshana, and S. Ruhman (to be published).
[56] B. J. Schwartz and P. J. Rossky, Phys. Rev. Lett. **72**, 3282 (1994).
[57] We note that the rate k_1 decreases slightly at bluer excitation wavelengths, consistent with the idea that additional internal electronic relaxation is required before detachment can occur, as suggested by the simulations in Ref. 29.
[58] V. Tran and B. J. Schwartz, J. Phys. Chem. B **103**, 5570 (1999); D. Aherne, V. Tran, and B. J. Schwartz, *ibid.* **104**, 5382 (2000).
[59] P. Clifford, N. J. B. Green, and M. J. Pilling, J. Phys. Chem. **86**, 1318 (1982).